T. SADOWSKI[*], E. ZARZEKA-RACZKOWSKA[*]

HYBRID ADHESIVE BONDED AND RIVETED JOINTS – INFLUENCE OF RIVET GEOMETRICAL LAYOUT ON STRENGTH OF JOINTS

POŁĄCZENIA HYBRYDOWE KLEJOWO-NITOWE – WPŁYW GEOMETRII ROZMIESZCZENIA NITÓW NA WYTRZYMAŁOŚĆ POŁĄCZEŃ

The hybrid adhesive bonded and riveted joints have wider and wider application in different branches of engineering: aerospace, mechanical, civil etc. The hybrid joints' strength is 1.5 to 3 times higher than only adhesive bonded joints' strength. The hybrid joints characterize higher reliability during long-term working.

In this article we present the influence of rivets' lay-out geometry on the hybrid adhesive bonded/riveted joints response to mechanical loading.

Experimental research was carried using 3-D digital image correlation system ARAMIS. This system enables monitoring of the deformation processes of the hybrid joint specimen up to failure. We analysed the state of deformation of the adhesive bonded double-lap joints reinforced by different numbers of rivets. The hybrid joint specimens were subjected to the uniaxial tensile test. Moreover, the influence of geometry of individual number of rivets' layout (rivets arranged in one or more rows) for hybrid joint strength was studied.

Experimental research was completed and supported by the computer simulations of the whole deformation processes of metal layers (aluminum), adhesive layers and rivets. Numerical simulations were conducted with the ABAQUS programme. The analysis of stress concentrations in different parts of the hybrid joint and their behaviour up to failure were investigated.

Finally, the analysis and the comparison of the obtained results confirmed the influence of rivets' lay-out geometry not only on rivets joints but also on the hybrid adhesive bonded/riveted joints.

Keywords: hybrid joint, adhesive joint, rivet joint, damage, FEA

Połączenia hybrydowe klejowo-nitowe znajdują coraz szersze zastosowania w różnych dziedzinach inżynieryjnych: mechanice, lotnictwie, inżynierii lądowej i innych. Mają one 1,5 – 3 razy większą wytrzymałość niż wytrzymałość połączeń wyłącznie klejowych oraz charakteryzują się większą niezawodnością w długotrwałej eksploatacji.

W niniejszym artykule przedstawiono wpływ geometrii rozmieszczenia nitów na wytrzymałość połączeń hybrydowych klejowo-nitowych poddanych jednoosiowemu rozciąganiu.

Badania eksperymentalne zostały przeprowadzone z zastosowaniem systemu monitoringu procesu deformacji ARAMIS, który pozwala na śledzenie tego procesu aż do momentu zniszczenia próbki. Wyznaczono stany deformacji w połączeniach klejowych dwunakładowych wzmocnionych różną ilością nitów poddanych jednoosiowemu rozciąganiu. Ponadto badano wpływ geometrii rozmieszczenia poszczególnej liczby nitów (szwy jedno- i wielorzędowe) na wytrzymałość połączenia hybrydowego.

Badania eksperymentalne zostały uzupełnione i potwierdzone symulacją komputerową zachodzących procesów zniszczenia w warstwach blach, kleju oraz nitach. Symulacje komputerowe przeprowadzono w programie ABAQUS.

Analiza i porównanie otrzymanych wyników potwierdzają wpływ geometrii rozmieszczenia nitów na wytrzymałość nie tylko połączeń nitowych, ale również połączeń typu hybrydowego.

1. Introduction

The continues requirement of improvements structural parts of engineering construction to meet better reliability and durability leads to application of new and innovative composite materials with different internal structure. The introduction of the porosity (e.g. [1-3]) or plastic matrix (e.g. [4-7]) to the composite modifies significantly their properties. In case of adhesive bonded joints of the structural elements one can observe application of the new types adhesives, which contains nanoparticles (e.g., carbon nanotubes [8], SiO_2 nanoparticles [9]

[*] FACULTY OF CIVIL ENGINEERING AND ARCHITECTURE, DEPARTMENT OF SOLID MECHANICS, LUBLIN UNIVERSITY OF TECHNOLOGY, 20-618 LUBLIN, 40 NADBYSTRZYCKA STR., POLAND

or graphene) to modify specific properties (e.g. electric conductivity [8, 9]). This adhesive layer can be treated as particle reinforced composite. Other possibility is to create a new composite material with gradual changes of physical and mechanical properties, i.e. production of so-called functionally graded material – FGM (e.g. [10-14]). In the pure adhesive joints this idea was applied in a form of mixed adhesive, i.e. by introduction of plastic and elastic region (with different stiffness) in the adhesive to increase joint strength by minimizing the maximum adhesive stress [15, 16].

The further improvement of the structural elements joining technology is to combine two simple joining techniques [17-21]. One can distinguish rivet-adhesive (e.g. [21-23]) and clinch-adhesive joints (e.g. [23-29]), spot-welded-adhesive joints etc. These modern technologies are used not only in aerospace but also in other branches of engineering [20-32]. The hybrid joints' strength can be 1.5 to 3 times higher than only adhesive bonded joints' strength. They have also higher reliability during the whole lifetime and under cyclic loading. One can distinguish three types of hybrid adhesive bonded and riveted joints: adhesive joints with a small number of rivets, rivet joints where the adhesive fulfills a gasket function and joints, in which both adhesive strength and rivet strength play part. The objective of the present research is description of the last type of joints.

The main problem to be analyzed in this paper is estimation of an influence of rivet geometrical layout on the hybrid adhesive bonded/riveted joints response to mechanical loading. The state of deformation and local stress concentrations of the adhesive bonded double-lap joints reinforced by three rivets is presented. In order to underline the advantage of the hybrid joints with comparison to the pure adhesive and the pure riveted joints the experimental and numerical analyses where performed.

2. Uniaxial tension tests

The experimental research was carried out using 3-D Digital Image Correlation (DIC) system ARAMIS. We have investigated double – lap hybrid adhesive bonded/riveted joints which were subjected to the uniaxial tensile tests. An aluminum plate and two aluminum laps (aluminum 1050A) were connected by the adhesive and rivets. We used the standard rivets which diameter is equal to 3.2 mm in aluminum body and steel mandrel. The thickness of the adhesive layers, made of Loctite 435^{TM}, was found after the curing about 0.1 mm. The details of the sample dimensions are presented in the Fig. 1.

Additionally, the pure adhesive bonded joints and the pure rivet joints were analysed to compare their mechanical properties with corresponding hybrid joints. The experiments show that the adhesive joints are working well till about 7 kN load and then fail suddenly. The maximum displacement is equal to 1.3 mm. The rivet joints for small riveting area behave in a similar way irrespective of the rivet geometrical layout. The difference in results is about 3% as for tensile force and from 3% to 9% as for displacement, type 1+2 rivet layout and longitudinal layout, respectively (Fig. 3).
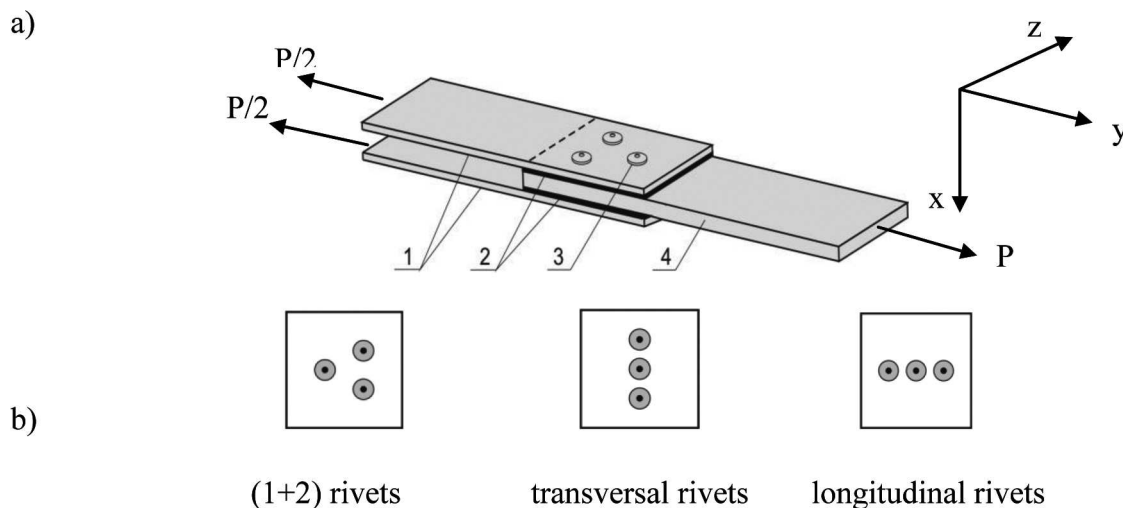

Fig. 1. a) Schematic picture of the hybrid joint with its geometry: **1** – two aluminum laps 40 x 130 x 2 mm; **2** – two adhesive layers 40 x 40 x 0,1 – 0,2 mm, **3** – rivets d = 3,2 mm, **4** – aluminum plate 40 x110 x 4 mm, b) Different geometry of rivet layout in rivets joints and hybrid adhesive bonded/riveted joints for three rivets
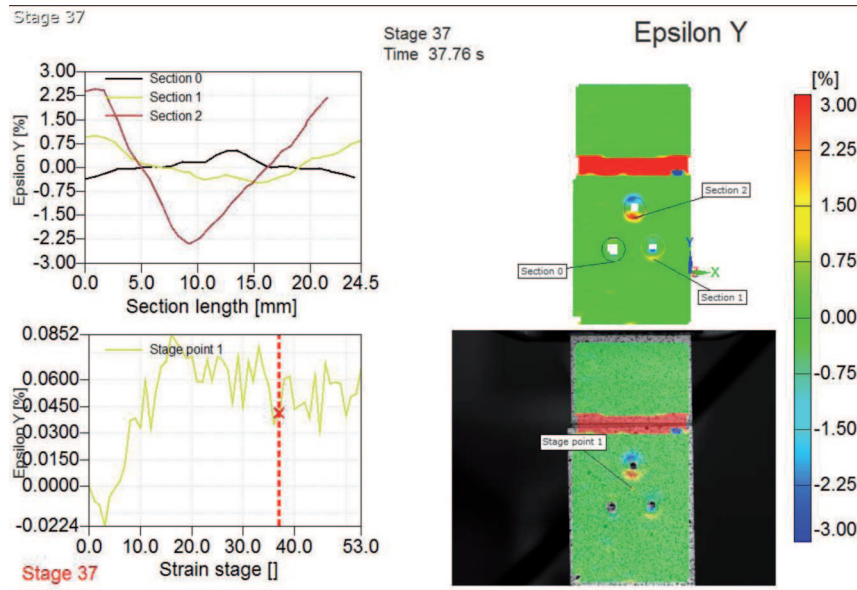
Fig. 2. Raport from measurement by the DIC system in hybrid adhesive bonded/riveted joint with type (1+2) rivets layout – relative elongation in cross sections around rivets (r = 2,5 mm)

The experimental results concerning the hybrid adhesive bonded/riveted joints were presented in Figs. 3-4. DIG system was applied for testing enables monitoring continuously the strain distributions at the hybrid joint surface. One can estimate the total sample mechanical response and especially we can distinguish the most strenuous rivet in the joint (Fig. 2). Diagrams present relative elongations distribution around rivets for the exemplary "stage 37" of deformation process (left top plot) and in some selected points in the rivets region (left bottom plot). This stage of deformation was marked also in Fig. 3. It corresponds to the advanced stage of deformation process after the adhesive failure in the joint.
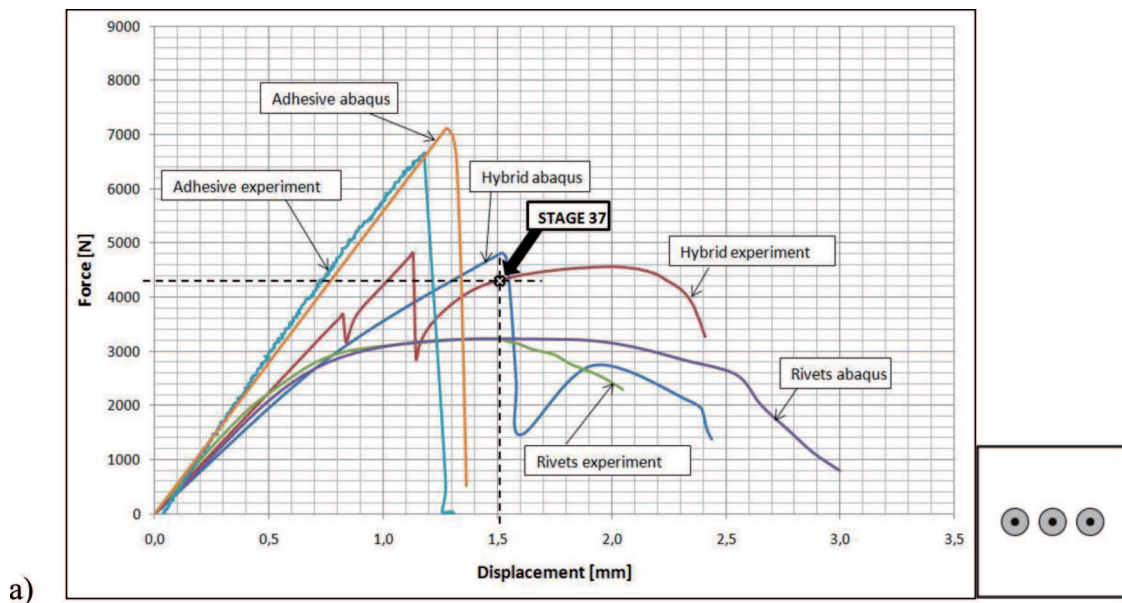
a)
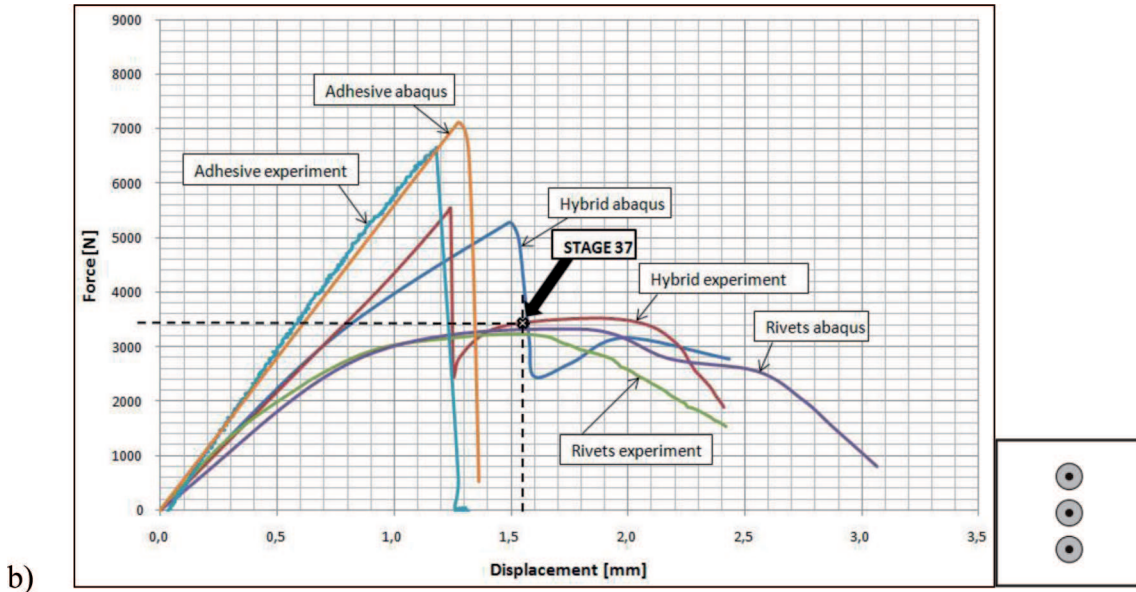
b)
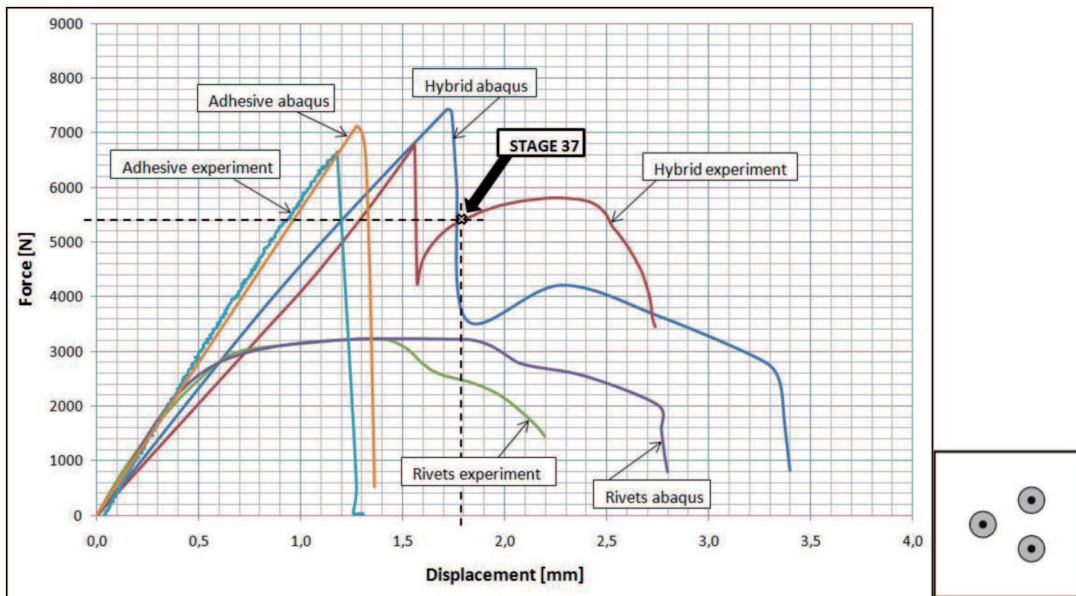
c)

Fig. 3. Comparison of the force - displacement tests respectively for each type of three rivets joint (a) with longitudinal rivets layout, b) with transverse rivets layout, c) with type (1+2) rivets layout) in two cases: experimental and numerical tests

3. Numerical investigation

The most general anisotropic damage evolution is described by a quadratic nominal stress criterion, e.g. [25-31], [33-40]:

$$\left\{\frac{\langle\sigma_n\rangle}{\sigma_{I,max}}\right\}^2 + \left\{\frac{\sigma_s}{\sigma^s_{II,\,max}}\right\}^2 + \left\{\frac{\sigma_t}{\sigma^t_{II,\,max}}\right\}^2 = 1, \quad (1)$$

where: $\langle\sigma_n\rangle = \sigma_n$ for $\sigma_n > 0$ or $\langle\sigma_n\rangle = 0$ for $\sigma_n < 0$ and $\sigma_{I,\,max}$, $\sigma^s_{II,\,max}$, $\sigma^t_{II,\,max}$ are the threshold values of

the damage initiation for simple modes of loading. The criterion (1) simplifies for the case of isotropic damage, then $\sigma_{I,\,max} = \sigma^s_{II,\,max} = \sigma^t_{II,\,max} = \sigma_{max}$.

The failure criterion, in the most general anisotropic case, was formulated as a power law (e.g. [35-40]):

$$\left\{\frac{G_I}{G_{Ic}}\right\}^\alpha + \left\{\frac{G_{II}}{G_{IIc}}\right\}^\alpha + \left\{\frac{G_{III}}{G_{IIIc}}\right\}^\alpha = 1, \quad (2)$$

and it depends on the energy release rate in three considered simple modes: I – normal, II and III – shear ones. Here α is an empirical parameter derived from tests,

$\alpha = 1 - 2$. G_{Ic}, G_{IIc}, G_{IIIc} are critical energy release rates for pure Mode I, Mode II and Mode III, respectively. In the simplest case, the fracture process can be isotropic and then:

$$G_{Ic} = G_{IIc} = G_{IIIc} = G_{Tc}, \qquad (3)$$

where G_{Tc} corresponds to the Mode I critical energy release rate.

The Finite Element Analysis (FEA), package ABAQUS, was used to predict the strength and deformations of rivets (R), adhesive bonded (A) and hybrid (H) joints subjected to the axial tensile loading up to the final failure.

The aluminum adherents and the rivets were subjected to large plastic deformations during monotonic uniaxial loading process. Their mechanical response was described by the Huber – von Mises yield model with the isotropic hardening.

The adhesive layers were modelled by application of cohesive elements (e.g. [22-29, 41, 42], which behave elastically until the damage initiation at σ_{max} for Mode I loading. In our calculations we assumed that $\sigma_{I,max} = \sigma_{II,max}^{s} = \sigma_{II,max}^{t} = 15$ MPa and the fracture energy is equal to $G_{Ic} = G_{IIc} = G_{IIIc} = 30$ N/m. We assumed these values on the basis of received experimental data (the force – displacement diagram). The parameter α in equation (2) is equal to 2.

Numerical simulation allows to observe and analyse of damage and failure processes in the interior parts of a joint (Figs. 4 – 5). We can see in particular that failure processes in the adhesive layers of all presented types of hybrid joints progress not at the same time. Adhesive failure started near specimen edges but if we compare stress concentrations in the adhesive layers for the step time for example equal to 2.8 which corresponds to 1.6 mm displacement, we can observe that one of the adhesive layer fail faster visibly, especially for hybrid joints with type 1+2 rivets layout and hybrid joints with transversal rivets layout. This nonsymmetrical failure of the adhesive layers also appears for the hybrid joints with longitudinal rivets layout (Fig. 5c, 5b, 5c). We can explain this effect by technology of joining because the lower part of a joint is squeezed more by a rivet head.

The individual diagrams (Fig. 3) present a comparison between adhesive joints, hybrid adhesive bonded/riveted joints and rivet joints for different types of rivet geometrical layout. Computing about tensile strength shows that the hybrid (H) joint (1+2) rivet layout type is a better connection of parts than pure adhesive (A) joint (H/A = 104%) or rivet (R) joint (H/R = 231%). The hybrid joint for longitudinal and transversal rivet layout types are worse joints than pure adhesive joint (H/A ~ 70%) and better than rivet (R) joint (H/R ~ 150%). Absorption of energy in all types of hybrid joints is bigger than in pure adhesive joints or rivet joints, [7]. Moreover, the hybrid joint (1+2) rivet layout type absorb the most energy of all types of hybrid joints – 42% more than hybrid longitudinal joint and 50% more than hybrid transversal joint (Tab. 1).

One can observe difference between the experimental curve and the numerical results. The main explanation of this phenomenon comes from lack of exact experimental data concerning critical values of G_{IIc} and G_{IIIc}. Both values were assumed to be equal to G_{Ic} according to (3). Moreover, in the next step of FEM analysis it is necessary to take into account damage processes which develop in plastic parts of the hybrid joint.
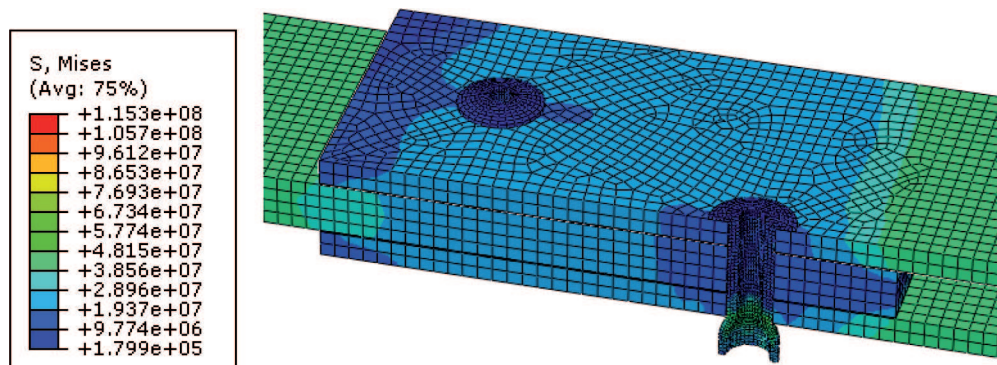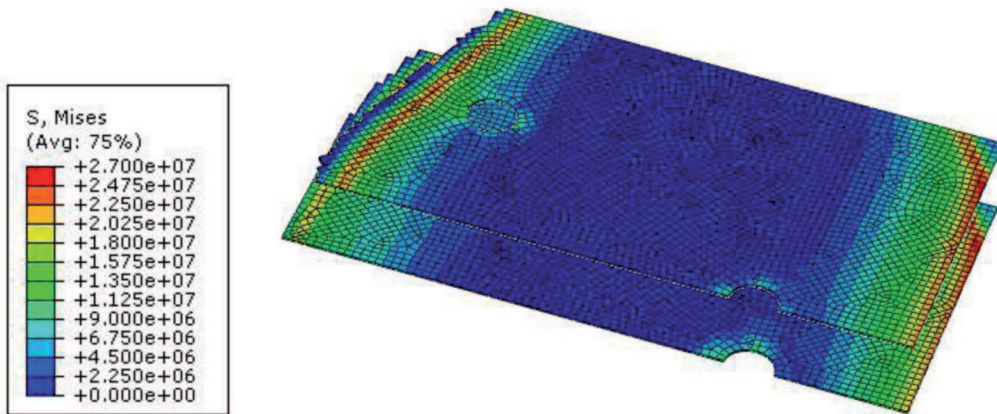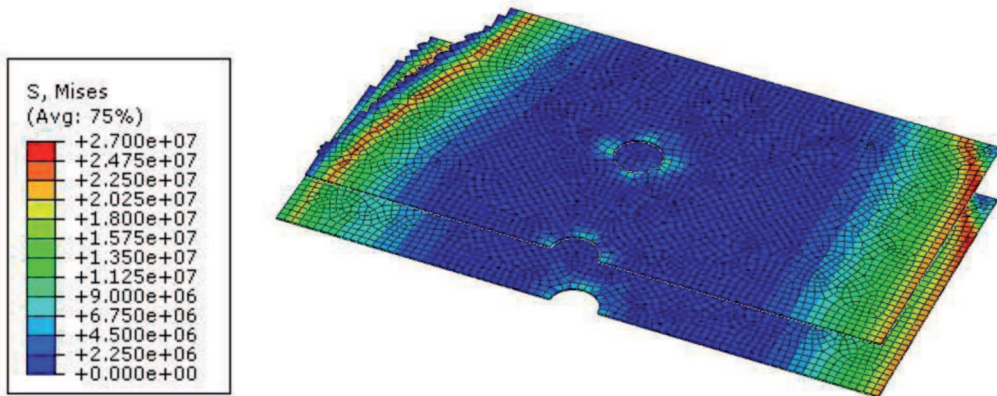

Fig. 4. Various types of elements were used to create the FEA model: C3D8R and C3D6 for aluminum plates and rivets, R3D3 and R3D4 elements for steel substrates of the rivets (for mandrels), COH3D8 and COH3D6 elements for adhesive layers. The total number of used elements was about 41 000
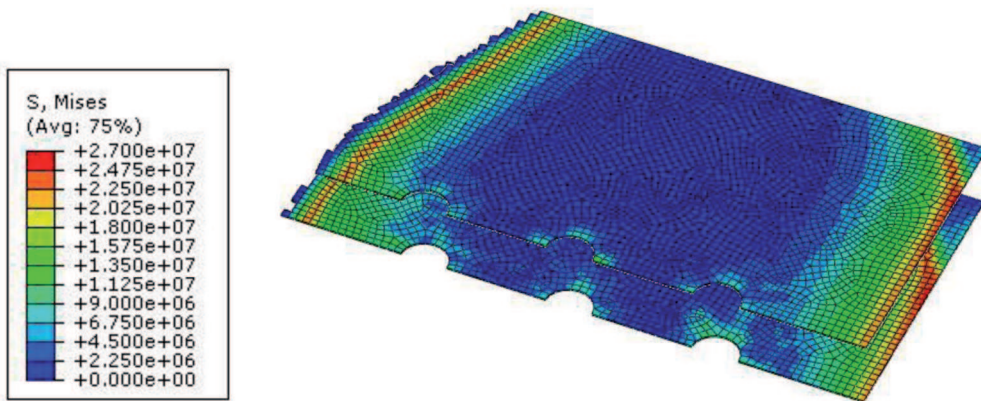
1132

a)

b)

c)

Fig. 5. Stress distribution in the adhesive layers in the hybrid adhesive bonded/riveted joint for the step time equal to 2.8 seconds (displacement 1.6 mm): a) with type (1+2) rivets layout, b) with transverse rivets layout, c) with longitudinal rivets layout

TABLE 1

Energy absorption in all types of joints (R, A, H) according to experimental and numerical researches

TYPE OF JOINT			ENERGY ABSORBTION [10^{-3}J]		
			Before max shearing force	After max shearing force	Total
HYBRID LONGTUDINAL		Experiment	2,312	5,762	8,074
		Abaqus	4,630	2,266	6,896
HYBRID TRANSVERSAL		Experiment	3,500	3,700	7,200
		Abaqus	4,420	2,890	7,310
HYBRID 1+2		Experiment	4,940	6,030	10,970
		Abaqus	8,324	4,140	12,464
ADHESIVE		Experiment	4,040	0,390	4,430
		Abaqus	4,290	0,284	4,574
RIVETS	LONGTUDINAL	Experiment	2,570	2,040	4,610
		Abaqus	3,440	3,196	6,636
	TRANSVERSAL	Experiment	3,320	2,410	5,730
		Abaqus	3,450	3,720	7,170
	1+2	Experiment	3,290	2,160	5,450
		Abaqus	3,750	3,500	7,250

4. Conclusions

In this paper the problem of the influence of three rivets geometrical layout on the strength of the hybrid adhesive bonded/riveted joints was investigated. Comparing the experimental results and numerical simulation for the adhesive bonded joints, the rivet joints and the hybrid joints for each rivet geometrical layout types (using three rivets), we can infer that the hybrid joints with rivet layout 1+2 is the best solution for joining structural parts. In this case after initial linear increase of the load – displacement curve, the samples curried the maximum force at the displacement of approximately equal to 1.6 mm. For the rest of cases of the rivet geometrical layout the maximum forces correspond to the displacement equal from 1.1 mm to 1.2 mm. The subsequent sudden reduction of force in the hybrid joints is the result of the adhesive failure. After that, only rivets carry the force up to the moment of failure. The rivets layout 1+2 makes the hybrid joint better tighten near the edges of the sample. Moreover, the distribution of the rivets in the lap region is more homogeneous, than for other cases. It results in the better joining of the adherents and strength of the adhesive in this type of joint. We can also observe the most regular strain distributions around the rivets. The tensile strength of the hybrid joint is about 3% higher than the analogous adhesive bonded joint and about 112% higher than the rivet joint only (Fig. 3c). What is the most important the energy absorption to final failure of the specimen is 1.7 times higher in comparison to purely adhesive joint and 1.4 higher in relation to only riveted joint (Tab. 1). Additionally, numerical simulations show the influence of a kind of riveting technology on a rate and coincidence of adhesive layer failure in hybrid joints (Fig 4, Fig. 5).

While in the hybrid adhesive bonded/riveted joints three types of rivet geometrical layout have essential influence on the joint strength, there is no so significant influence on the joint strength in the pure rivet joints with three different types of rivets layout (Fig. 3).

Computer simulation shows about 80% compatibility of the numerical model with the experiments (Fig. 3).

REFERENCES

[1] T. S a d o w s k i, S. S a m b o r s k i, Prediction of mechanical behaviour of porous ceramics using meso-

1134

mechanical modelling. Comput. Mat. Sci. **28**, 512-517 (2003).

[2] T. Sadowski, S. Samborski, Modelling of porous ceramics response to compressive loading. J. Am. Cer. Soc. **86**, 2218-2221 (2003).

[3] T. Sadowski, S. Samborski, Development of damage state in porous ceramics under compression. Comput. Mat. Sci. **43**, 75-81 (2008).

[4] T. Sadowski, S. Hardy, E. Postek, Prediction of the mechanical response of polycrystalline ceramics containing metallic inter-granular layers under uniaxial tension. Comput. Mat. Sci. **34**, 46-63 (2005).

[5] T. Sadowski, S. Hardy, E. Postek, A new model for the time-dependent behaviour of polycrystalline ceramic materials with metallic inter-granular layers under tension. Mat. Sci. Eng. A **424**, 230-238 (2006).

[6] T. Sadowski, E. Postek, Ch. Denis, Stress distribution due to discontinuities in polycrystalline ceramics containing metallic inter-granular layers. Comput. Mat. Sci. **39**, 230-236 (2007).

[7] T. Sadowski, T. Nowicki, Numerical investigation of local mechanical properties of WC/Co composite, Comput. Mat. Sci. **43**, 235-241 (2008).

[8] Z. Wu, J. Li, D. Timmer, K. Lorenzo, S. Bose, Study of processing variables on the electrical resistivity of conductive adhesives, Int. J. Adhes. & Adhes. **29**, 488-494 (2009).

[9] H. Zhao, T. Liang, B. Liu, Synthesis and properties of copper conductive adhesives modified by SiO$_2$ nanoparticles, Int. J. Adhes. & Adhes. **27**, 429-433 (2007).

[10] T. Sadowski, M. Boniecki, Z. Librant, K. Nakonieczny, Theoretical prediction and experimental verification of temperature distribution in FGM cylindrical plates subjected to thermal shock. Int. J. Heat and Mass Transfer **50**, 4461-4467 (2007).

[11] T. Sadowski, S. Ataya, K. Nakonieczny, Thermal analysis of layered FGM cylindrical plates subjected to sudden cooling process at one side – comparison of two applied methods for problem solution, Comp. Mater. Sci, **45**, 624-632 (2009).

[12] T. Sadowski, A. Neubrand, Estimation of the crack length after thermal shock in FGM strip, Int. J. Fract. **127**, 135-140 (2004).

[13] K. Nakonieczny, T. Sadowski, Modelling of thermal shock in composite material using a meshfree FEM, Comp. Mater. Sci. **44**, 1307-1311 (2009).

[14] T. Sadowski, K. Nakonieczny, Thermal shock response of FGM cylindrical plates with various grading patterns, Comput. Mat. Sci. **43**, 171-178 (2008).

[15] L.F.M. da Silva, P.J.C. das Neves, R.D. Adams, J.K. Spelt, Analytical models of adhesively bonded joints – Part I: Literature survey, Int. J. Adhes. & Adhes. **29**, 319-330, (2009).

[16] L.F.M. da Silva, P.J.C. das Neves, R.D. Adams, J.K. Spelt, Analytical models of adhesively bonded joints – Part II: Comparative study, Int. J. Adhes. & Adhes. **29**, 331-341, (2009).

[17] A.V. Pocius, Adhesion and adhesives technology, Hasner, New York (1997).

[18] R.D. Adams, J. Comyn, W.C. Wake, Structural adhesive joints in engineering. 2nd ed. Chapman&Hall, London (1997).

[19] L.F.M. da Silva, A. Öchsner (Eds), Modelling of adhesively bonded joints, Springer (2008).

[20] L.F.M. da Silva, A. Öchsner, R.D. Adams, Handbook of Adhesion Technology, Springer (2011).

[21] L.F.M. da Silva, A. Öchsner, A. Pirondi (Eds), Hybrid adhesive joints, Springer (2011).

[22] T. Sadowski, M. Kneć, P. Golewski, Experimental investigations and numerical modelling of steel strip adhesive joint reinforced by rivets, Int. J. Adhes. & Adhes. **30**, 338-346 (2010).

[23] T. Sadowski, P. Golewski, E. Zarzeka-Raczkowska, Damage and failure processes of hybrid joints: Adhesive bonded aluminum plates reinforced by rivets, Comput. Mat. Sci. **50**, 1256-1262 (2011).

[24] F. Moroni, A. Pirondi, F. Kleiner, Experimental analysis and comparison of the strength of simple and hybrid structural joints, Int. J. Adhes. & Adhes. **30**, 367-379 (2010).

[25] A. Pirondi, F. Moroni, Clinch-bonded and rivet-bonded hybrid joints: application of damage models for simulation of forming and failure, J. Adhes. Sci. Technol. **23**, 1547-1574 (2009).

[26] T. Sadowski, T. Balawender, Technology of Clinch – Adhesive Joints, in Hybrid adhesive joints. Advanced Structured Materials, **6**, Springer 2011, L. F. M. da Silva, A. Pirondi, A. Öschner (Eds), 149-176.

[27] T. Balawender, T. Sadowski, P. Golewski, Experimental and numerical analyses of clinched and adhesively bonded hybrid joints, J. Adhes. Sci Technol. **25**, 2391-2407 (2011).

[28] T. Balawender, T. Sadowski, M. Knec, Technological problems and experimental investigation of hybrid: clinched – adhesively bonded joint, Arch. Metall. Mat. **56**, 439-446 (2011).

[29] T. Balawender, T. Sadowski, P. Golewski, Numerical analysis and experiments of the clinch-bonded joint subjected to uniaxial tension, Comput. Mat. Sci. **64**, 270-272 (2012).

[30] S. Gómez, J. Oñoro, J. Pecharromán, A simple mechanical model of a structural hybrid adhesive/riveted single-lap joint, J. Int. J. Adhes. & Adhes. **27**, 263-267 (2007).

[31] G. Kelly, Load transfer in hybrid (bonded/bolted) composite single-lap joint Compos. Struct. **69**, 35-43 (2005).

[32] T.A. Barnes, I.R. Pashby, Joining techniques for aluminum spaceframes esed in automobiles. Part II. Adhesive bonding and mechanical fasteners, J. Mater. Process. Technol. **99**, 72-79 (2000).

[33] A. Needleman, A continuum model for void nucleation by inclusion debonding, J. Appl. Mech. **54**, 525-531 (1987).

[34] V. T v e r g a a r d, J. H u t c h i n s o n, The relation between crack growth resistance and fracture process parameters in elastic-plastic solids, J. Mech. Phys. Solids **40**, 1377-1397 (1992).

[35] L. M a r s a v i n a, T. S a d o w s k i, Stress intensity factors for an interface kinked crack in a bi-material plate loaded normal to the interface. Int. J. Frac. **145**, 237-243 (2007).

[36] L. M a r s a v i n a, T. S a d o w s k i, Fracture parameters at bi-material ceramic interfaces under bi-axial state of stress. Comp. Mater. Sci. **45**, 693-697 (2009).

[37] T. S a d o w s k i, L. M a r s a v i n a, N. P e r i d e, E.-M. C r a c i u n, Cracks propagation and interaction in an orthotropic elastic material: analytical and numerical methods, Comput. Mat. Sci. **46**, 687-693 (2009).

[38] L. M a r s a v i n a, T. S a d o w s k i, Kinked cracks at a bi-material ceramic interface – numerical determination of fracture parameters. Comput. Mat. Sci. **44**, 941-950 (2009).

[39] T. S a d o w s k i, G. G o l e w s k i, Effect of aggregate kind and graining on modelling of plain concrete under compression, Comput. Mat. Sci. **43**, 119-126 (2008).

[40] E. P o s t e k, T. S a d o w s k i, Assessing the Influence of Porosity in the Deformation of Metal-Ceramic Composites, Composite Interfaces **18**, 57-76 (2011).

[41] V. B u r l a y e n k o, T. S a d o w s k i, Influence of skin/core debonding on free vibration behaviour of foam and honeycomb cored sandwich plates, Int. J. Non-Linear Mechanics **45**, 959-968 (2010).

[42] V. B u r l a y e n k o, T. S a d o w s k i, Analysis of structural performance of aluminum sandwich plates with foam-filled hexagonal foam, Comp. Mater. Sci. **45**, 658-662 (2009).